Low-energy level schemes of ^{66,68}Fe and inferred proton and neutron excitations across $Z = 28$ and $N = 40$

S. N. Liddick,[1,2] B. Abromeit,[1] A. Ayres,[3] A. Bey,[3] C. R. Bingham,[3] B. A. Brown,[1,4] L. Cartegni,[3] H. L. Crawford,[5] I. G. Darby,[6] R. Grzywacz,[3] S. Ilyushkin,[7] M. Hjorth-Jensen,[1,8,4] N. Larson,[1,2] M. Madurga,[3] D. Miller,[3] S. Padgett,[3] S. V. Paulauskas,[3] M. M. Rajabali,[6] K. Rykaczewski,[9] and S. Suchyta[1,2]

[1]*National Superconducting Cyclotron Laboratory (NSCL), Michigan State University, East Lansing, Michigan 48824, USA*
[2]*Department of Chemistry, Michigan State University, East Lansing, Michigan 48824, USA*
[3]*Department of Physics and Astronomy, University of Tennessee, Knoxville, Tennessee 37996, USA*
[4]*Department of Physics and Astronomy, Michigan State University, East Lansing, Michigan 48824, USA*
[5]*Nuclear Science Division, Lawrence Berkeley National Laboratory, Berkeley, California 94720, USA*
[6]*Instituut voor Kern- en Stralingsfysica, Katholieke Universiteit Leuven, B-3001 Leuven, Belgium*
[7]*Department of Physics and Astronomy, Mississippi State University, Mississippi 39762, USA*
[8]*Department of Physics and Center of Mathematics for Applications, University of Oslo, N-0316 Oslo, Norway*
[9]*Physics Division, Oak Ridge National Laboratory, Oak Ridge, Tennessee 37831, USA*

(Received 29 October 2012; revised manuscript received 11 December 2012; published 22 January 2013)

Background: The nuclei in the region around ^{68}Ni display an apparent rapid development of collectivity as protons are removed from the $f_{7/2}$ single-particle state along the $N = 40$ isotonic chain. Proton and neutron excitations across the $Z = 28$ and $N = 40$ gaps are observed in odd-A $_{27}$Co and $_{26}$Fe isotopes. Little spectroscopic information beyond the excited 2^+ and 4^+ is available in the even-even $^{66,68}_{26}$Fe nuclei to compare with shell model calculations.

Purpose: Our goal is to determine the low-energy level schemes of ^{66,68}Fe and compare the observed excitations with shell model calculations to identify states wherein a contribution from excitations across $Z = 28$ and $N = 40$ are present.

Method: The low-energy states of ^{66,68}Fe were populated through the beta decay of ^{66,68}Mn produced at the National Superconducting Cyclotron Laboratory. Beta-delayed gamma-ray transitions were detected and correlated to the respective parent isotope to construct a low-energy level scheme.

Results: The low-energy level schemes of ^{66,68}Fe were constructed from observed gamma-ray coincidences and absolute gamma-ray intensities. Tentative spin and parity assignments were assigned based on comparisons with shell model calculations and systematics. The two lowest 0^+ and 2^+ states were characterized in terms of the number of protons and neutrons excited across the respective shell gaps.

Conclusion: The removal of two protons from ^{68}Ni to ^{66}Fe results in an inversion of the normal configuration and the one characterized by significant excitation across the $Z = 28$ and $N = 40$ gaps. Approximately, one proton and two neutrons are excited across their respective single-particle gaps in the ground state of ^{66}Fe.

DOI: 10.1103/PhysRevC.87.014325 PACS number(s): 23.40.−s, 21.10.−k, 27.50.+e

I. INTRODUCTION

A significant experimental and theoretical effort has been directed at understanding the rapid development of collectivity below ^{68}Ni in the $N = 40$ region. The nucleus, ^{68}Ni, was originally thought to be located at the intersection of a proton shell closure at $Z = 28$ due to the isolated $f_{7/2}$ proton single-particle state and a neutron subshell closure at $N = 40$ resulting from the separation between the pf shell and the neutron $g_{9/2}$ single-particle state. Support for the semimagic interpretation of ^{68}Ni was originally derived from a high 2^+ excitation energy [1].

The view of ^{68}Ni as a closed core nucleus was challenged by the observation of a rapid drop in the energy of the first excited 2^+ states, $E(2^+_1)$, along the Fe and Cr isotopic chains without any pronounced peak at either $^{66}_{26}$Fe$_{40}$ [2] or $^{64}_{24}$Cr$_{40}$ [3]. Complementary $B(E2)$ measurements along the Fe [4] and Cr [5] isotopic chains also indicate the increased collectivity in this neutron-rich region. The development of collectivity has been attributed to the filling of the neutron $g_{9/2}$ single-particle state in $N < 40$ nuclei driving the nucleus toward deformation [2]. Excited states originating from neutron excitations from the pf shell into the neutron $g_{9/2}$ single-particle state across $N = 40$ are observed in all neutron-rich odd-A Fe isotopes starting at $N = 33$. Levels with tentative spin and parity assignments of $9/2^+$ have been identified in $^{59}_{26}$Fe$_{33}$ [6] and $^{61}_{26}$Fe$_{35}$ [7–9], and inferred in $^{63}_{26}$Fe$_{37}$ [9], $^{65}_{26}$Fe$_{39}$ [8–10], and $^{67}_{26}$Fe$_{41}$ [8,11], though in ^{67}Fe alternative positive parity states cannot be exclusively ruled out [12]. The $9/2^+$ levels in the odd-A Fe isotopes decrease from 1517 keV in ^{59}Fe to approximately 400 keV in both ^{65,67}Fe [10]. The monotonic decrease in the energy of the tentatively assigned $9/2^+$ levels in the odd-A Fe isotopes is mirrored in the Mn isotopic chain by the drop in the energy of the negative parity bandhead associated with the coupling of the $\pi f_{7/2}$ and $\nu g_{9/2}$ single-particle states approaching $N = 40$ [13].

Removing one proton from $Z = 28$ leaves a vacancy in the $f_{7/2}$ single-particle orbital resulting in a $7/2^-$ ground state spin and parity assigned to all neutron-rich odd-A Co

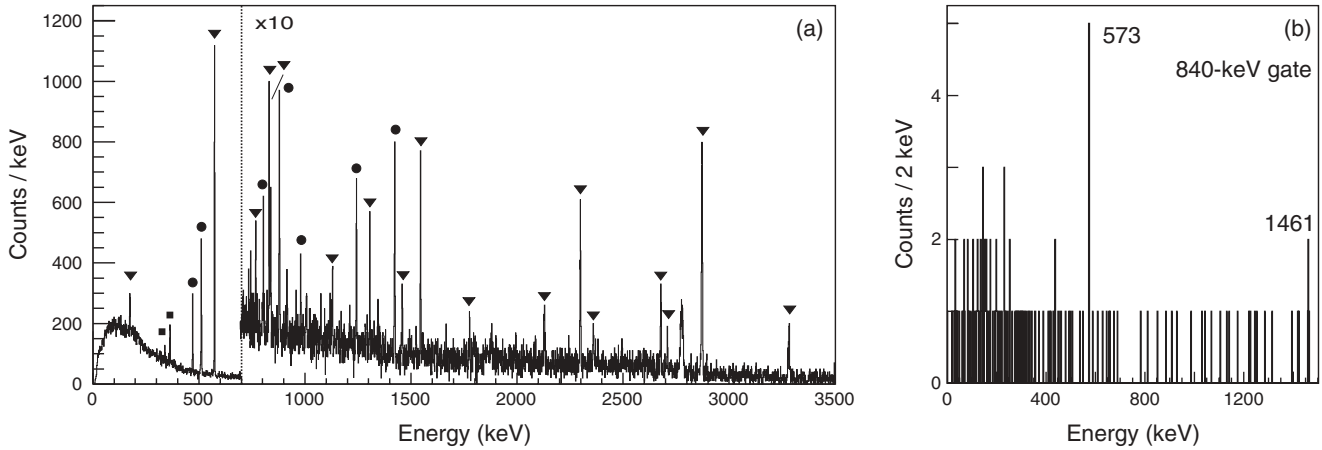

FIG. 1. (a) The beta-delayed gamma-ray energy spectrum observed within 500 ms following the implantation of a ^{66}Mn ion. Gamma rays attributed to the decay of ^{66}Mn are labeled with inverted triangles and are listed in Table I. Gamma rays attributed to daughter and granddaughter activities are marked by circles. Gamma rays associated with the decay of nuclei populated through beta-delayed neutron emission are indicated by squares. The unlabeled "peak" at approximately 2800 keV is due to the overflow signal on one of the individual SeGA detectors. (b) The gamma-gamma coincidence spectrum gated by the 840-keV transition. Coincidences with the 573- and 1461-keV transitions are indicated.

isotopes. The presence of intruder levels have been observed in the odd-A ^{65,67}Co isotopes wherein proton excitations across the $Z = 28$ shell have been suggested to account for the anomalous low-energy $1/2^-$ states in both ^{65,67}Co [14,15]. States associated with both normal and intruder configurations have also been tentatively identified in the odd-odd ^{66,68}Co [16] and ^{64,66}Mn [17] isotopes located on either side of $N = 40$. The identification of both proton and neutron intruder levels sparked a renewed interest in identifying corresponding states in the even-even ^{68}Ni nucleus, and theoretical predications were put forward for the excitation energy of the proton two-particle two-hole 0^+ state in ^{68}Ni [18]. Despite initial indications [19] the state has not yet been identified [20].

In order to extend the search for normal and intruder configurations below the $_{28}$Ni isotopic chain requires more extensive knowledge of the level schemes of the even-even ^{66,68}Fe nuclei.

II. EXPERIMENTAL DESCRIPTION AND RESULTS

The level schemes of the neutron-rich $^{66,68}_{26}$Fe isotopes were investigated through the beta decay of the respective Mn isotopes to identify levels above the previously reported tentative 2^+ and 4^+ [2,21] states for comparison with shell model calculations. The neutron-rich ^{66,68}Mn ions were produced at the Coupled Cyclotron Facility at the National Superconducting Cyclotron Laboratory (NSCL) by impinging a 140 MeV/A ^{86}Kr primary beam on a ^{9}Be target. The fragmentation products of interest were separated using the A1900 [22] and delivered to the central implantation detector of the Beta Counting System (BCS) [23] which was surrounded by 16 detectors from the Segmented Germanium Array (SeGA) [24]. Both systems were instrumented with the NSCL DDAS [25]. Further details on the experimental setup and the characterization of the ions delivered to the experimental station can be found in Refs. [16,17].

The beta-delayed gamma-ray spectrum observed within 500 ms following the arrival of a ^{66}Mn ion to the experimental station is shown in Fig. 1(a). The 573-keV and 834-keV transitions have been observed previously in Refs. [2,9,21]. Gamma-ray transitions up to an energy of 3.3 MeV are are observed in Fig. 1(a), assigned to the decay of ^{66}Mn, and are listed in Table I with their respective absolute intensities. The beta decay curve for ^{66}Mn is shown in Fig. 2. The half-lives of the daughter ^{66}Fe and granddaughter ^{66}Co were fixed at 351 ms [17,26–28] and 180 ms [27,29,30] respectively. The errors on the daughter (6 ms) and granddaughter (10 ms) half-lives did not contribute significantly to the error of the extracted ^{66}Mn half-life. The half-life determined for ^{66}Mn from the present data is 60(3) ms, consistent with previous measurements of 65(5) [12], 64(2) [31], and 66(4) ms [2]. Gamma-gated decay curves for the most intense photon transitions were also analyzed and were consistent with the overall beta-decay curve. The 573-keV gamma-gated decay curve is shown as an inset in Fig. 2. A small beta-delayed neutron branch was observed following the decay of ^{66}Mn based on the presence of the 363.5-keV transition associated with ^{65}Fe [8,10,32].

TABLE I. Energies and absolute intensities for the gamma-ray transitions identified following the beta decay of ^{66}Mn.

E (keV)	Abs. inten. (%)	E (keV)	Abs. inten. (%)
175.2 (2)	3.6 (6)	1777.5 (4)[a]	2 (1)
573.4 (1)	38 (2)	2130.4 (6)[a]	5 (2)
770.2 (2)	1.4 (6)	2300.2 (2)	7 (1)
833.9 (2)	3.5 (6)	2362.0 (6)[a]	2 (1)
840.4 (3)	1.7 (6)	2680.0 (3)	6 (2)
1132.8 (3)	1.1 (5)	2710.4 (4)	1.3 (7)
1307.6 (2)	1.8 (9)	2874.0 (2)	16 (2)
1461.2 (3)	1.0 (7)	3284.5 (5)	6 (2)
1547.5 (2)	5.5 (8)		

[a]Not placed in level scheme.

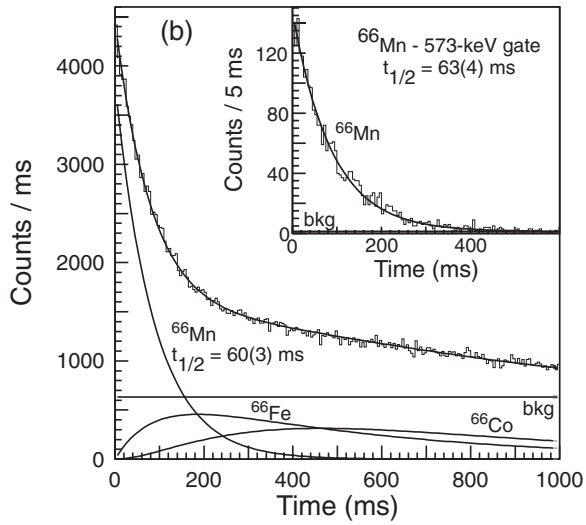

FIG. 2. The beta-decay curve for ^{66}Mn from 0 to 1 second. The overall fit was composed of contributions from the beta decay of ^{66}Mn, ^{66}Fe, ^{66}Co, and a constant background. Inset: The beta-decay curve for ^{66}Mn from 0 to 600 ms detected in coincidence with the observation of a 573-keV gamma ray.

The 340.5-keV transition in the beta-delayed gamma-ray spectrum follows the decay of ^{65}Fe [15] populated in the delayed neutron emission from ^{66}Mn. The coincident 882-keV transition following the 340-keV transition was not observed due to the drop in efficiency between the two photon energies. The beta-delayed neutron branch was not considered in the half-life fit due to its small magnitude of 4(1)%.

Numerous gamma-gamma coincidence spectra were obtained and the gamma coincidence spectra obtained with a gate on the 840-keV transition is shown in Fig. 1(b). Based on observed gamma-gamma coincidences and absolute gamma-ray intensities the low-energy level scheme of ^{66}Fe populated in the beta-decay of ^{66}Mn was constructed and is shown in Fig. 3, which is consistent with the level scheme constructed from the decay of ^{66}Mn produced through proton-induced U fission at ISOLDE [33]. Apparent beta-decay feedings are listed to the left of each level and a Q value of 13.32 MeV was assumed for the calculations of $\log_{10} ft$ values according to Ref. [34]. The spin and parity of the ^{66}Mn parent ground state has been tentatively assigned as 1^+ [17] and thus the beta decay from ^{66}Mn will preferentially populate low-spin states in the ^{66}Fe daughter nucleus. Shell model calculations are presented next to the level scheme in Fig. 3 and will be discussed in more detail later in the paper. In the cases where the ordering of transitions from coincidence data was ambiguous, the order was based on absolute intensities with the highest absolute intensity transition at the bottom of the respective gamma-ray cascade.

The beta-delayed gamma-ray spectrum observed within 300 ms following the implantation of a ^{68}Mn ion is presented in Fig. 4(a). A total of four gamma rays were attributed to the decay of ^{68}Mn at 521.2 (1), 865.3 (2), 1249.5 (4), and 1513.7 (3) keV with absolute intensities of 43(5), 24(5), 13(5), and 14(4), respectively. The two low-energy transitions at 521- and 865-keV have been observed previously [12,21]. The ^{68}Mn decay curve is shown in Fig. 4(b). The decay curve

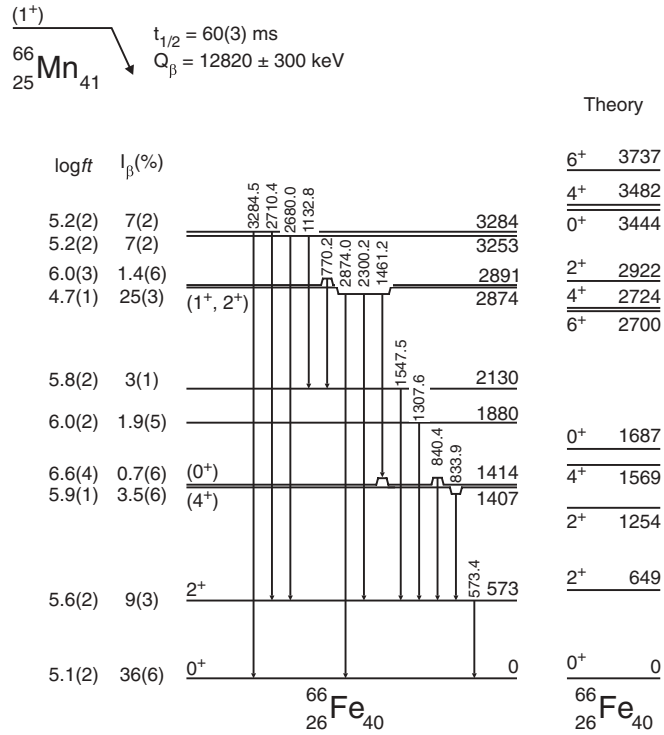

FIG. 3. (Left) Low-energy level scheme of ^{66}Fe inferred from the beta decay of ^{66}Mn. Tentative spin and parity assignments, apparent beta-decay branching ratios, and $\log_{10} ft$ values are given on the left hand side of each state. The beta-decay Q value was taken from a recent mass measurement [35]. (Right) Shell model calculations for ^{66}Fe; see text for details.

was fit with contributions from ^{68}Mn, ^{68}Fe, and ^{68}Co. The half-lives of ^{68}Fe and ^{68}Co were fixed at values of 180 [16] and 1600 ms [29] respectively. The half-life of ^{68}Mn was determined to be 40(7) ms, slightly shorter than obtained previously, 51(4) ms [12], but with a lower precision.

The inferred low-energy level scheme of ^{68}Fe is presented in Fig. 5 with apparent beta-decay feedings from ^{68}Mn. The levels at 521 and 1386 keV are shown as solid lines and were previously identified in Ref. [12], but the present data allows for the determination of apparent beta decay feedings to each state. Based on the similarity in the observed absolute gamma-ray intensities for the 1249.5 and 1513.7 keV states it is tempting to place the two gamma rays in a cascade which feeds the 521-keV level indicated by dashed lines in Fig. 5. The order of the 1249.5–1513.7 keV cascade could not be conclusively determined.

III. DISCUSSION

To explore the structure of the neutron-rich Fe isotopes, shell model calculations were performed using an effective interaction derived with the techniques detailed in Refs. [36]. The N^{3}LO model of Entem and Machleidt [37] was used for the nucleon-nucleon interaction and to construct an effective interaction appropriate for Fe isotopes with ^{48}Ca used as a reference state. All terms in many-body perturbation to third order in the renormalized interaction were included, in

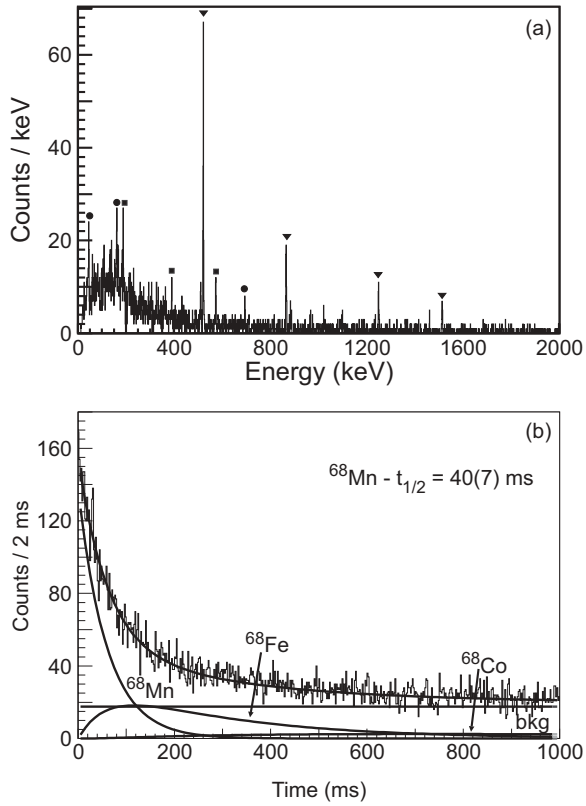

FIG. 4. (a) The beta-delayed gamma-ray energy spectrum detected within 300 ms following a ^{68}Mn implanted ion. Gamma rays attributed to the decay of ^{68}Mn are labeled with inverted triangles. Gamma rays attributed to daughter and granddaughter activity are marked by circles. Gamma rays associated with the decay of nuclei populated following beta-delayed neutron emission are indicated by squares. (b) The beta-decay curve for ^{68}Mn from 0 to 1 second. The overall fit (black) was composed of contributions from the beta-decay of ^{68}Mn, ^{68}Fe, ^{68}Co, and a constant background.

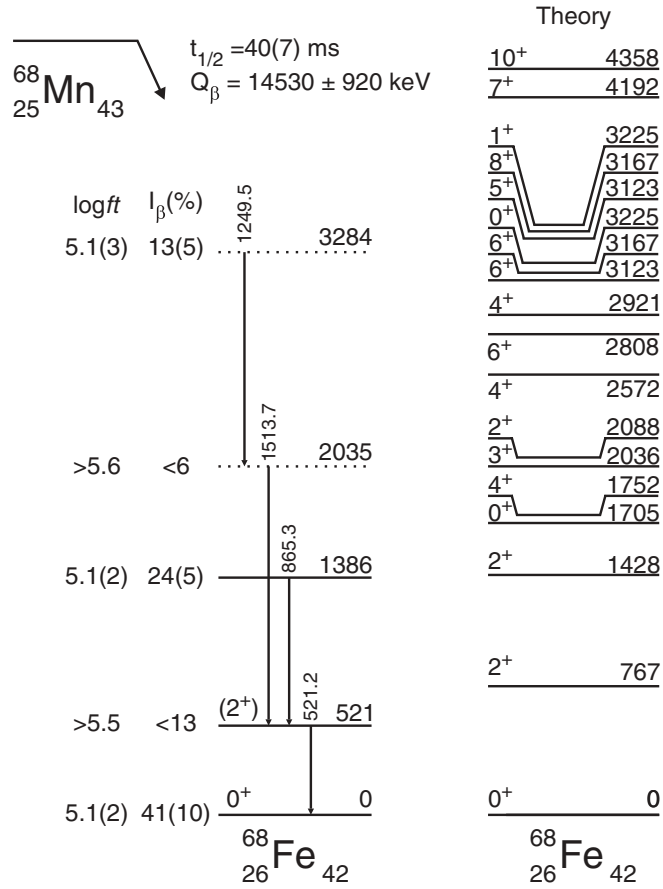

FIG. 5. (Left) Low-energy level scheme of ^{68}Fe inferred from the beta decay of ^{68}Mn. Beta-decay branching ratios and apparent $\log_{10} ft$ values are given on the left-hand side of each state. The beta-decay Q value of the decay was taken as 14 530 keV from Ref. [34]. (Right) Shell model calculations for ^{68}Fe; see text for details. All calculated states below 3.5 MeV are shown. Above 3.5 MeV only the lowest excited states of a given spin and parity are shown.

addition to folded diagrams which were summed to infinite order. A G matrix was computed with respect to ^{48}Ca as a closed core employing an oscillator basis with oscillator energy $\hbar\omega = 10$ MeV; see Ref. [36] for further details. The effective interaction for the shell model space consists of the proton single-particle states $0f_{7/2}$, $0f_{5/2}$, $1p_{3/2}$, and $1p_{1/2}$ and the neutron single-particle states $0f_{5/2}$, $1p_{3/2}$, $1p_{1/2}$, and $0g_{9/2}$. To minimize the computational complexity of the shell model calculations, a maximum of two proton excitations were allowed out of the $f_{7/2}$ single-particle state. No limitation was placed on the number of neutron excitations amongst the given states. The single-particle energies were initially set to empirical values relevant for ^{49}Sc and ^{49}Ca. It is likely that monopole corrections will be required to reproduce the effective values for the $A = 66$ region. The only adjustment that was made was to shift the neutron $g_{9/2}$ single-particle energy so that the observed excitation energies in ^{65}Fe and ^{66}Fe were reasonable. It may be that this adjustment was not a unique solution. In addition it is thought that the neutron $d_{5/2}$ orbital is important to obtain the proper correlation energies in this region [38]. Thus, the present shell model calculations are at a rather early stage and are used only for qualitative guidance in the interpretation of the present results.

The predicted ground state spin and parity of ^{66}Mn is 1^+ in agreement with the inferred spin and parity obtained in Ref. [17]. The shell model calculations additionally predict a 32% beta-decay branch between the ground state of ^{66}Mn and the 0^+ ground state of ^{66}Fe compared with a 36(6)% ground state branch inferred in the present work. The first excited 2^+ state in ^{66}Fe, depopulated by a 573.4-keV transition, was observed in prior beta-decay and reaction studies [2,3,12,21] and is confidently assigned as the $2_1^+ \rightarrow 0^+$ transition. A 4^+ spin and parity assignment is given to the state at 1407 keV. The 834-keV transition observed in beta decay agrees with the similar energy transitions observed in both knockout [833(9) keV] [21] and inelastic scattering reactions [831(8) keV] [3]. The 1407-keV state is also populated through beta-delayed neutron emission from from the tentative $5/2^-$ ^{67}Mn ground state from the present data. The large beta-decay Q value for ^{66}Mn and the possibility of missing high-energy low-intensity transitions suggest that the apparent feeding of the 1407-keV state is an upper limit and could be lowered if additional

transitions are identified in future experiments. The 834-keV transition was not observed in the previous beta-decay work of Ref. [2] due to a contaminant line at 833.5 keV from ^{66}Ga. The 957-keV transition observed in the knockout reactions is likely the $6^+ \rightarrow 4^+$ transition and was not observed in the beta decay.

The 1414-keV state is tentatively identified as an excited 0^+ state in ^{66}Fe based on the lack of an observed 1414-keV crossover transition, the absence of observable feeding from higher excited states, and a comparison to shell model calculations. The predicted beta-decay intensity to the excited 0^+ state is 0.1% compared to an experimentally measured 0.7(6)%.

A comparison between the experimental and theoretical level schemes of ^{68}Fe in Fig. 5 is more difficult due to the lack of experimentally observed transitions. The spin and parity of the parent ^{68}Mn nucleus was assumed to be greater than 3 based on the beta-decay feeding of the assumed 4_1^+ state in ^{68}Fe [12]. The present shell model calculations predict the spin and parity of the parent ^{68}Mn nucleus to be 0^+ with 1^+ and 2^+ excited states at energies of 161 and 191 keV, respectively. The next excited state in ^{68}Mn is a 5^+ level located at 471 keV. The large apparent ground state beta-decay feeding observed in the decay of ^{68}Mn is inconsistent with a higher-spin assignment to the ground state of ^{68}Mn. The 0^+ spin and parity assignment predicted by the shell model calculations can also be excluded based on the large beta-decay branch ratio to the ground state of ^{68}Fe. Thus there is a slight preference from the experimental data for either the 1^+ or 2^+ spin and parity assignment. However, if the decay is fragmented across numerous high-energy states that subsequently emit low-intensity high-energy photons directly to the ground state, the inferred beta-decay feeding to the ground state would be lower and further experimental data is required to verify the large ground state branch.

The occupation probabilities for the low-energy 0^+ and 2^+ excited states in $^{68}_{28}$Ni, $^{66}_{26}$Fe, and $^{68}_{26}$Fe were taken from the shell model calculations and the number of protons excited out of the $f_{7/2}$ single-particle state across the $Z = 28$ gap, and the number of neutrons excited into the $g_{9/2}$ single-particle state across the $N = 40$ gap were determined and are presented in Fig. 6. For ^{68}Fe the number of excited neutrons refers to the number of additional neutrons excited in the $g_{9/2}$ single-particle state in excess of the two expected in a normal filling configuration. The 0^+ ground state of ^{68}Ni is the nearest to a closed shell configuration with only 0.44 and 0.26 protons and neutrons excited across $Z = 28$ and $N = 40$ energy gaps, respectively. The number of protons and neutrons excited across their respective single-particle energy gaps at $Z = 28$ and $N = 40$ is significantly higher for the 0_2^+ and 0_3^+ states in $^{68}_{28}$Ni$_{40}$. The trend is similar for the 0^+ states in $^{68}_{26}$Fe$_{42}$; the ground state appears to have relatively little excess neutron excitation in the $g_{9/2}$ single-particle state while the excited

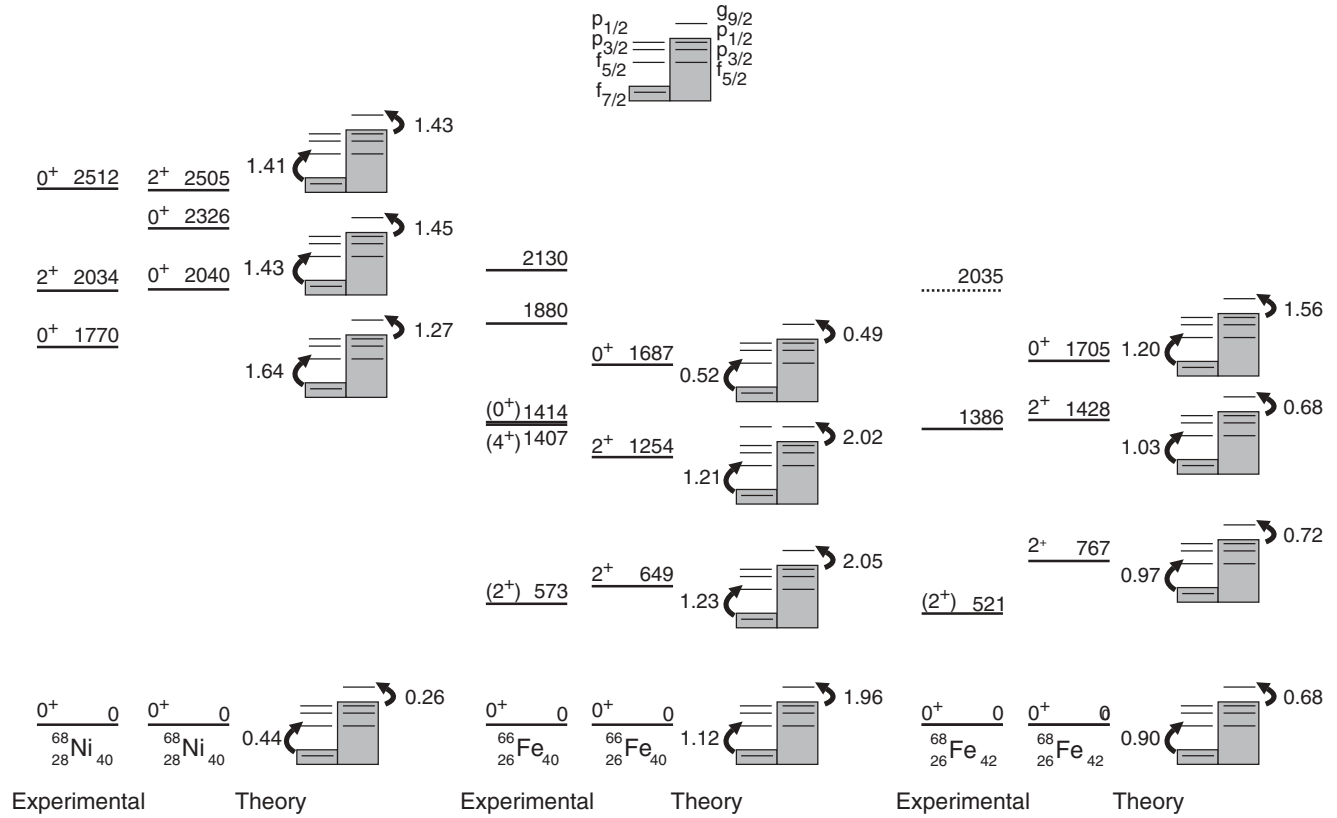

FIG. 6. Comparisons between the experimental level schemes below 2.5 MeV with the calculated energies for the low-energy 0^+ and 2^+ states in $^{68}_{28}$Ni$_{40}$, $^{66}_{26}$Fe$_{40}$, and $^{68}_{26}$Fe$_{42}$. The model space used in the calculations is shown at the top of the figure. For the calculated states, the number of protons excited out of the $f_{7/2}$ single-particle state and the the number of neutrons excited into the $g_{9/2}$ single-particle state are shown schematically to the right of the theoretical state. See text for details.

0^+ state predicted at 1705 keV shows almost an extra two neutrons excited into the $g_{9/2}$ single-particle state.

Based on the theoretical calculations the intruder configuration drops below the normal one in ^{66}Fe with the ground state involving an average excitation of 1.12 protons and 1.96 neutrons across $Z = 28$ and $N = 40$, respectively. The closed shell configuration in ^{66}Fe is found at an excitation energy of 1414 keV and is associated with the second 0^+ state predicted theoretically. The dramatic change in the number of excited nucleons across the respective single-particle energy gaps was also found in previous theoretical studies [38,39]. Our present calculations predict slightly different values for the number of neutrons excited into the $g_{9/2}$ single-particle state; 0.26 versus 0.96 in Ref. [38] for ^{66}Fe and 1.96 versus 3.17 in Ref. [38] for ^{68}Fe. The differences are likely attributable to the limitations that have been placed on the model used in the present work. However, the overall conclusion remains unchanged. The ground state of ^{66}Fe is dominated by particle-hole configurations.

IV. SUMMARY

In conclusion, the low-energy level schemes of the neutron-rich ^{66,68}Fe isotopes were studied through the beta decay of the respective Mn isotopes. For the decays of ^{66,68}Mn, absolute beta-decay branching ratios were determined and used to restrict spins and parities of selected states populated in the beta decay. Additionally, the low-energy level schemes of ^{66,68}Fe were compared with shell model calculations taking into account neutron excitation into the the $g_{9/2}$ single-particle state and proton excitations across the $Z = 28$ gap. A tentative 0^+ excited state was observed in ^{66}Fe which appears to have a closed shell configuration similar to the ground state of ^{68}Ni based on comparisons with shell model calculations. The energy of the intruder configurations involving significant proton and neutron excitations across the $Z = 28$ and $N = 40$ gaps drops in energy between ^{68}Ni and ^{67}Co, becoming the ground state in ^{66}Fe.

ACKNOWLEDGMENTS

This work was funded in part by the NSF under Contracts No. PHY-1102511 (NSCL) and No. PHY-1068217, and by the DOE under Contracts No. DE-FG02-96ER40983 (UT), No. DE-AC05-00OR22725 (ORNL), No. DE-AC05-060R23100 (ORAU), No. DE-FC03-03NA00143 (NNSA), and No. DE-NA0000979 (NNSA).

[1] R. Broda, B. Fornal, W. Królas, T. Pawłat, D. Bazzacco, S. Lunardi, C. Rossi-Alvarez, R. Menegazzo, G. de Angelis, P. Bednarczyk, J. Rico, D. De Acuña, P. J. Daly, R. H. Mayer, M. Sferrazza, H. Grawe, K. H. Maier, and R. Schubart, Phys. Rev. Lett. **74**, 868 (1995).
[2] M. Hannawald, T. Kautzsch, A. Wöhr, W. B. Walters, K.-L. Kratz, V. N. Fedoseyev, V. I. Mishin, W. Böhmer, B. Pfeiffer, V. Sebastian, Y. Jading, U. Köster, J. Lettry, and H. L. Ravn, Phys. Rev. Lett. **82**, 1391 (1999).
[3] A. Gade *et al.*, Phys. Rev. C **81**, 051304 (2010).
[4] W. Rother *et al.*, Phys. Rev. Lett. **106**, 022502 (2011).
[5] T. Baugher *et al.*, Phys. Rev. C **86**, 011305 (2012).
[6] E. K. Warburton, J. W. Olness, A. M. Nathan, J. J. Kolata, and J. B. McGrory, Phys. Rev. C **16**, 1027 (1977).
[7] N. Vermeulen *et al.*, Phys. Rev. C **75**, 051302 (2007).
[8] R. Grzywacz *et al.*, Phys. Rev. Lett. **81**, 766 (1998).
[9] S. Lunardi *et al.*, Phys. Rev. C **76**, 034303 (2007).
[10] M. Block, C. Bachelet, G. Bollen, M. Facina, C. M. Folden III, C. Guenaut, A. A. Kwiatkowski, D. J. Morrissey, G. K. Pang, A. Prinke, R. Ringle, J. Savory, P. Schury, and S. Schwarz, Phys. Rev. Lett. **100**, 132501 (2008).
[11] M. Sawicka *et al.*, Eur. Phys. J. A **16**, 51 (2003).
[12] J. M. Daugas *et al.*, Phys. Rev. C **83**, 054312 (2011).
[13] C. J. Chiara, I. Stefanescu, N. Hoteling, W. B. Walters, R. V. F. Janssens, R. Broda, M. P. Carpenter, B. Fornal, A. A. Hecht, W. Królas, T. Lauritsen, T. Pawłat, D. Seweryniak, X. Wang, A. Wöhr, J. Wrzesiński, and S. Zhu, Phys. Rev. C **82**, 054313 (2010).
[14] D. Pauwels, O. Ivanov, N. Bree, J. Büscher, T. E. Cocolios, J. Gentens, M. Huyse, A. Korgul, Y. Kudryavtsev, R. Raabe, M. Sawicka, I. Stefanescu, J. Van de Walle, P. Van den Bergh, P. Van Duppen, and W. B. Walters, Phys. Rev. C **78**, 041307 (2008).
[15] D. Pauwels *et al.*, Phys. Rev. C **79**, 044309 (2009).
[16] S. N. Liddick, B. Abromeit, A. Ayres, A. Bey, C. R. Bingham, M. Bolla, L. Cartegni, H. L. Crawford, I. G. Darby, R. Grzywacz, S. Ilyushkin, N. Larson, M. Madurga, D. Miller, S. Padgett, S. Paulauskas, M. M. Rajabali, K. Rykaczewski, and S. Suchyta, Phys. Rev. C **85**, 014328 (2012).
[17] S. N. Liddick *et al.*, Phys. Rev. C **84**, 061305 (2011).
[18] D. Pauwels, J. L. Wood, K. Heyde, M. Huyse, R. Julin, and P. Van Duppen, Phys. Rev. C **82**, 027304 (2010).
[19] A. Dijon *et al.*, Phys. Rev. C **85**, 031301 (2012).
[20] C. J. Chiara *et al.*, Phys. Rev. C **86**, 041304 (2012).
[21] P. Adrich, A. M. Amthor, D. Bazin, M. D. Bowen, B. A. Brown, C. M. Campbell, J. M. Cook, A. Gade, D. Galaviz, T. Glasmacher, S. McDaniel, D. Miller, A. Obertelli, Y. Shimbara, K. P. Siwek, J. A. Tostevin, and D. Weisshaar, Phys. Rev. C **77**, 054306 (2008).
[22] D. J. Morrissey, B. M. Sherrill, M. Steiner, A. Stolz, and I. Wiedenhoever, Nucl. Instrum. Methods Phys. Res., Sect. B **204**, 90 (2003).
[23] J. I. Prisciandaro, A. C. Morton, and P. F. Mantica, Nucl. Instrum. Methods Phys. Res., Sect. A **505**, 140 (2003).
[24] W. F. Mueller, J. A. Church, T. Glasmacher, D. Gutknecht, G. Hackman, P. G. Hansen, Z. Hu, K. L. Miller, and P. Quirin, Nucl. Instrum. Methods Phys. Res., Sect. A **466**, 492 (2001).
[25] K. Starosta, C. Vaman, D. Miller, P. Voss, D. Bazin, T. Glasmacher, H. Crawford, P. Mantica, H. Tan, W. Hennig, M. Walby, A. Fallu-Labruyere, J. Harris, D. Breus, P. Grudberg, and W. Warburton, Nucl. Instrum. Methods Phys. Res., Sect. A **610**, 700 (2009).
[26] S. Leenhardt *et al.*, Nucl. Phys. A **654**, 683c (1999).
[27] O. Sorlin *et al.*, Nucl. Phys. A **660**, 3 (1999).
[28] F. Ameil, M. Bernas, P. Armbruster, S. Czajkowski, P. Dessagne, H. Geissel, E. Hanelt, C. Kozhuharov, C. Miehe, C. Donzaud,

A. Grewe, A. Heinz, Z. Janas, M. de Jong, W. Schwab, and S. Steinhäuser, Eur. Phys. J. A **1**, 275 (1998).
[29] W. F. Mueller *et al.*, Phys. Rev. C **61**, 054308 (2000).
[30] S. Czajkowski, M. Bernas, P. Armbruster, H. Geissel, C. Kozhuharov, G. Munzenberg, D. Vieira, P. Dessagne, C. Miehe, E. Hanelt, G. Audi, and J. K. P. Lee, Z. Phys. A **348**, 267 (1994).
[31] O. Sorlin *et al.*, Nucl. Phys. A **719**, C193 (2003).
[32] J. M. Daugas *et al.*, in *Frontiers in Nuclear Structure, Astrophysics, and Reactions: FINUSTAR, Kos, Greece, 2005*, edited by S. Harissopulos, P. Demetriou, and R. Julin, AIP Conf. Proc. No. 831 (AIP, New York, 2006), p. 427.
[33] D. Pauwels, contributed at ARIS 2011, Advances in Radioactive Isotope Science, Leuven, Belgium 2011 (unpublished).
[34] G. Audi, A. Wapstra, and C. Thibault, Nucl. Phys. A **729**, 337 (2003), the 2003 NUBASE and Atomic Mass Evaluations.
[35] S. Naimi, G. Audi, D. Beck, K. Blaum, C. Böhm, C. Borgmann, M. Breitenfeldt, S. George, F. Herfurth, A. Herlert, A. Kellerbauer, M. Kowalska, D. Lunney, E. Minaya Ramirez, D. Neidherr, M. Rosenbusch, L. Schweikhard, R. N. Wolf, and K. Zuber, Phys. Rev. C **86**, 014325 (2012).
[36] M. Hjorth-Jensen, T. T. Kuo, and E. Osnes, Phys. Rep. **261**, 125 (1995).
[37] R. Machleidt and D. Entem, Phys. Rep. **503**, 1 (2011).
[38] S. M. Lenzi, F. Nowacki, A. Poves, and K. Sieja, Phys. Rev. C **82**, 054301 (2010).
[39] K. Kaneko, Y. Sun, M. Hasegawa, and T. Mizusaki, Phys. Rev. C **78**, 064312 (2008).